BIOCHEMISTRY
including biophysical chemistry & molecular biology

Article

pubs.acs.org/biochemistry

Structure and Orientation of the gH625−644 Membrane Interacting Region of Herpes Simplex Virus Type 1 in a Membrane Mimetic System

Stefania Galdiero,[†,‡,§,#] Luigi Russo,[∥,#] Annarita Falanga,[†] Marco Cantisani,[†,‡] Mariateresa Vitiello,[⊥] Roberto Fattorusso,[∥,‡] Gaetano Malgieri,[∥] Massimiliano Galdiero,[‡,⊥] and Carla Isernia*[,‡,∥]

[†]Department of Biological Sciences, Division of Biostructures, and [‡]Centro Interuniversitario di Ricerca sui Peptidi Bioattivi, University of Naples "Federico II", Napoli, Italy

[§]Istituto di Biostrutture e Bioimmagini − CNR, Napoli, Italy

[∥]Department of Environmental Sciences, Second University of Naples, Caserta, Italy

[⊥]Department of Experimental Medicine, Second University of Naples, Napoli, Italy

Supporting Information

ABSTRACT: Glycoprotein H (gH) of the herpes simplex virus type 1 is involved in the complex mechanism of membrane fusion of the viral envelope with host cells. The virus requires four glycoproteins (gB, gD, gH, gL) to execute fusion and the role played by gH remains mysterious. Mutational studies have revealed several regions of gH ectodomain required for fusion and identified the segment from amino acid 625 to 644 as the most fusogenic region. Here, we studied the behavior in a membrane-mimicking DPC micellar environment of a peptide encompassing this region (gH625−644) and determined its NMR solution structure and its orientation within the micelles.

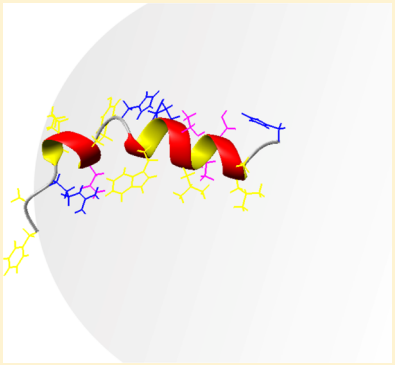

The entry of enveloped viruses into host cells relies on the fusion between the viral and host cell membranes, and it is controlled by one or more viral surface proteins (fusion proteins) that undergo conformational changes that drive membrane fusion.[1] The physical event needed to promote membrane fusion induced by enveloped viruses is the insertion of fusion peptides from one of the viral proteins into the cellular membrane to disrupt the normal organization of the lipids in their vicinity. Herpes simplex virus (HSV), unlike many enveloped viruses that induce fusion through the activity of a single viral fusion protein, requires four glycoproteins—glycoprotein B (gB), glycoprotein D (gD), glycoprotein H (gH), and glycoprotein L (gL)—to execute fusion.[2−4] Viral attachment is mediated by the binding of glycoprotein C (gC) or gB to cell surface glycosaminoglycans such as heparan sulfate.[5] The subsequent fusion between the virion envelope and host cell membrane is believed to be the result of a series of concerted events in which the required HSV glycoproteins work together to accomplish fusion. The detailed mechanism of HSV penetration into cells is still obscure; nonetheless, it is clear that gH and gB are key contributors of the fusion event, and both gB and gH/gL[6] are required for hemifusion and fusion.

The gB crystal structure has been solved,[7] showing structural homology to the postfusion structures of two known viral fusion proteins, indicating that, despite not being sufficient for HSV fusion, gB is likely a fusion protein. The role played by gH during fusion is still mysterious. Mutational studies have revealed several regions of the gH ectodomain that are required for fusion,[8] and a number of peptides matching different regions of the gH ectodomain have been shown to interact with membranes and proposed to play a role in the fusion process.[9,10] The recently solved crystal structure of HSV-2 gH/gL revealed a structure with no homology to any known fusion protein[11] and proposes a new model in which gH is required to either negatively or positively regulate the activity of gB through direct binding.[12]

We have previously demonstrated that synthetic peptides modeled on HSV-1 gH (gH220−262, gH381−420, gH493−537, gH626−644) are able to induce rapid membrane fusion.[13] We have also determined the structures of gH626−644 and gH617−644 in TFE/water mixtures and showed that both assume a well-defined helical structure.[9,10] More recently, we have shown that a peptide encompassing the stretch of gH comprising amino acids 625−644 represents the most fusogenic peptide, and it is very effective in inducing lipid mixing.[10,14] Its mechanism of translocation across the lipid

Received: October 17, 2011
Revised: February 8, 2012
Published: March 8, 2012

   dx.doi.org/10.1021/bi201589m | *Biochemistry* 2012, 51, 3121−3128

membrane is intriguing and the subject of intense studies because of its potential use for drug delivery across cell membranes.[14,15]

Since membrane−peptide systems are too large to allow the determination of the structure of a membrane bound peptide in its native environment, a determination of the structure of this fusogenic peptide in a membrane mimicking environment might therefore shed further light on its role in membrane fusion. In the present work, we have structurally characterized gH625−644 in a membrane-mimicking DPC micellar environment. We have used a ^{15}N-selective labeling of its residues to analyze the peptide behavior and orientation within the micelle.

EXPERIMENTAL SECTION

Peptide Synthesis. ^{15}N-Ala-labeled peptide (gH625−644: HGLASTLTRWAHYNALIRAF-COOH) was synthesized using standard solid-phase 9-fluorenylmethoxycarbonyl (Fmoc) method as previously reported.[10] The peptide was purified by HPLC and confirmed by mass spectral analysis.

Samples Preparation. gH625−644 is scarcely soluble in pure water. Two 1 mM sample solutions were prepared by dissolving ^{15}N-Ala-labeled lyophilized gH625−644 peptide in a volume of 500 μL of TFE. DPC-d38 was dissolved separately in 500 μL of water to obtain a 100 mM solution (DPC CMC = 1.1 mM).[16] Subsequently, the peptide solution was added gradually to the DPC solution, and water was added to yield a water/TFE 16:1 v/v ratio. The samples were lyophilized and then rehydrated with H_2O/D_2O (90/10 v/v). The final pH was then adjusted to 6. The micellar solutions prepared were stable over the time of the experiments (~1 month). In experiments using the external paramagnetic probe small amounts of aqueous solution of $MnCl_2$ were added to the peptide−micelle sample up to a 1/3 peptide/$MnCl_2$ molar ratio. 16-Doxylstearic acid (16-DSA) dissolved in methanol-d_4 was added to the second sample (detergent/spin-label, 63/1 molar ratio) for internal micellar mapping before peptide addition. D_2O (99.9% relative isotopic abundance), methanol-d_4 (99.96%), and DPC-d38 (98%) were purchased from Cambridge Isotope Laboratories. 16-DSA spin-label, TFE, and $MnCl_2$ were obtained from Sigma-Aldrich.

NMR Spectroscopy. NMR spectra were recorded at 300 K on a Varian Unity 500 MHz spectrometer. The proton chemical shifts were referenced to the residual TFE methylene resonance (3.88 ppm); ^{15}N chemical shifts were referenced indirectly. Two-dimensional ^{1}H−^{1}H TOCSY[17] and ^{1}H−^{1}H NOESY[18] spectra were recorded with mixing times of 80 and 150 ms, respectively. A spectral width of 6000 Hz was used in both dimensions. Squared shifted sine-bell functions were applied in both dimensions prior to FT. Water suppression was achieved using the DPFGSE sequence.[19] Two-dimensional ^{1}H−^{15}N HSQC, ^{15}N-filtered 2D TOCSY, and NOESY experiments were also recorded with mixing times of 70 and 100 ms. Data were processed and analyzed using the VNMRJ and CARA software.[20] ^{15}N{^{1}H} heteronuclear NOEs were determined from the ratio of signal intensities (I^{on}/I^{off}) in spectra recorded with and without the saturation of the amide protons for 3 s.

Structure Calculations. Conformational constraints for structure calculations were obtained from NOE-derived upper limit distances (Figure S1). Structure calculations were performed with the torsion angle dynamics CYANA program.[21,22] The final input for CYANA calculations was made up of 90 nonredundant upper distance constraints and 85 dihedral angle constraints. Among 100 calculated structures, the 20 with the lowest CYANA target function were chosen and refined by means of restrained energy minimization with the program SPdbV.[23] The absence of residual violations indicated that the constraints were well satisfied by the calculated structures and that the input data set was self-consistent (Table 1). The structures were visualized and evaluated using the programs MOLMOL[24] and PROCHECK-NMR.[25] The chemical shift assignments and the final atomic coordinates are available from the BioMagResBank (accession number: 18335) and from ProteinData Bank (PDB ID: 2lqy), respectively.

Table 1. Structural Statistics for the Final 20 Structures of gH625−644

quantity	value
NOE upper distance limits	90
dihedral angle constraints	85
residual target function, Å^2	0.13 ± 0.01
residual NOE violations, number > 0.1 Å, max, Å	0
residual angle violations, number >2.0°	0
% residues in the most favorable and additionally allowed region of the Ramachandran plot	97
% residues in the generously allowed region	3
rmsd to the mean coordinates, Å	
N, Cα, C′ (3−16)	0.274
all heavy atoms (3−16)	0.999

Diffusion Experiments. The hydrodynamic radius R_h was calculated from the translational diffusion coefficients, D_{trans}, by the Stokes equation. PFG diffusion measurements with the PG-SLED (pulse gradient-stimulated echo longitudinal encode-decode) sequence[26] permitted to obtain D_{trans}.[27] Each diffusion data set contained a series of 13 monodimensional ^{1}H spectra with gradient strength from 0.5 to 30 G/cm. D_{trans} data were obtained by DOSY package of the VNMRJ software. The hydrodynamic properties of the peptide in aqueous solution were also estimated by using HYDRO software.[28]

Tryptophan Quenching Experiments with Br-PC. Tryptophan is sensitive to its environment and has been previously utilized to evaluate peptide localization in the membrane. Emission spectra of gH625−644 in the absence or presence of target vesicles (PC/Chol = 55/45) were recorded between 300 and 400 nm with an excitation wavelength of 295 nm.

Br-PC employed as quencher of tryptophan fluorescence is suitable for probing membrane insertion of peptides, since it acts over a short distance and it does not drastically perturb the membrane.[29,30] The peptide was added (final concentration of 0.5 μM) to 2 mL of buffer (5 mM Hepes, 100 mM NaCl pH 7.4) containing 20 μL (50 mM) of Br-PC/Chol SUV, thus establishing a lipid:peptide molar ratio of 100:1. After a 2 min incubation at room temperature, an emission spectrum of the tryptophan was recorded with excitation set at 295 nm. SUV composed of PC/Chol (55/45) and containing 25% of either 6,7 Br-PC, 9,10 Br-PC, or 11,12 Br-PC were used. Three separate experiments were conducted. In control experiments, the peptide in PC/Chol (55/45) SUVs without Br-PC was used.

Fluorometric Detection of Membrane Pores. Pore-mediated diffusion potential was detected fluorometrically using the valinomycin-mediated diffusion potential assay.[31,32] 4 μL (28.8 μg) of SUVs made of PC/Chol (55/45), prepared

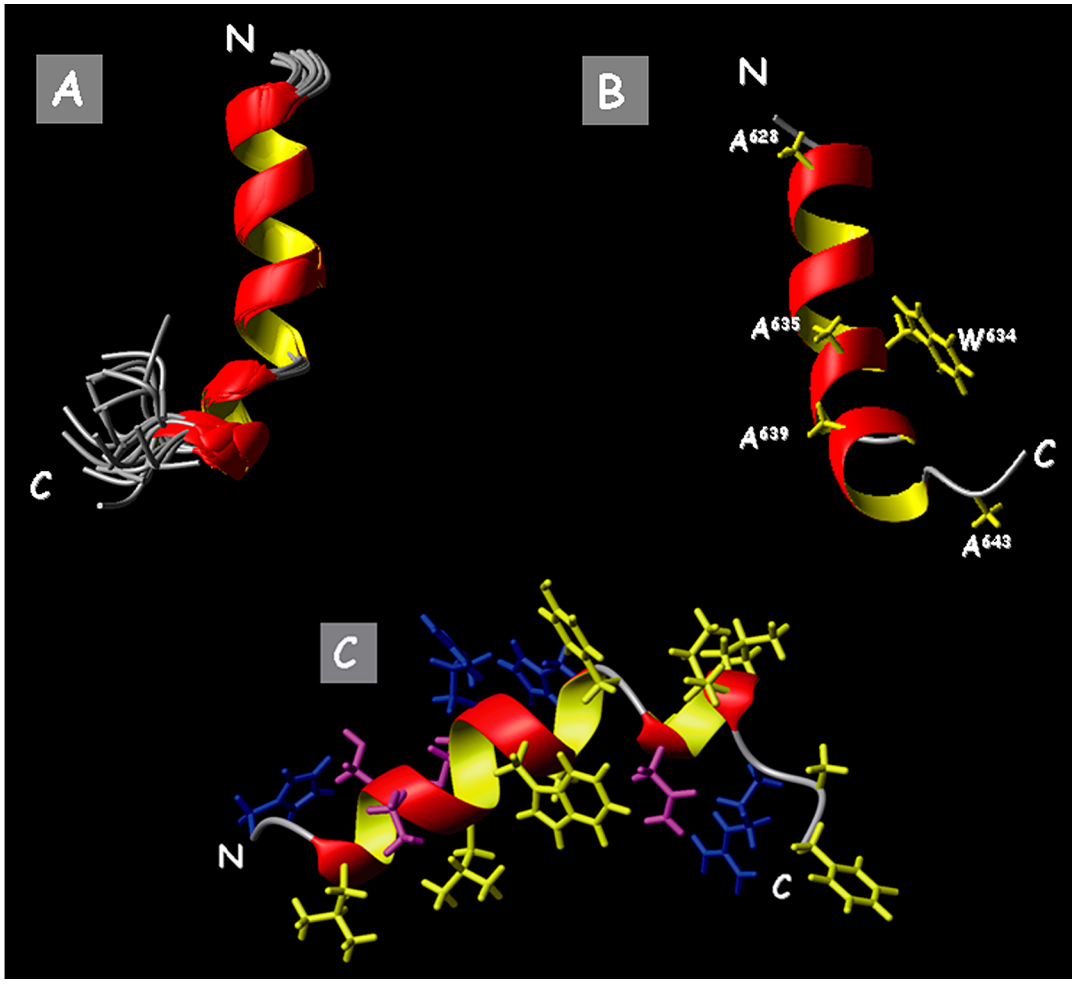

Figure 1. Backbone atoms superposition (residues 627−640) of the 20 energy-minimized structures of gH625−644 (A). Representative conformer of gH625−644 NMR structure (B); side chains of the four alanine residues and of the tryptophan are shown. The amphiphilic character of gH625−644 (C): charged residue side chains are in blue, polar in violet, and hydrophobic in yellow.

in K^+ buffer (50 mM K_2SO_4, 25 mM HEPES−SO_4^{2-}, pH 6.8), was added to 1 mL of isotonic K^+-free buffer (50 mM Na_2SO_4, 25 mM HEPES−SO_4^{2-}, pH 6.8), and the dye diS-C_2-(5) was added to get a final dye concentration of 1 μM. Subsequently, the addition of a valinomycin solution (final concentration 10^{-6} M) created a negative diffusion potential inside the vesicles by selectively carrying K^+ outside which caused an additional quenching of the dye's fluorescence. After the fluorescence was stable (10 min), the peptide was added. The permeation of the other ions (influx of Na^+ and efflux of SO_4^{2-}) and dissipation of the diffusion potential were monitored by the increase of the fluorescence with excitation at 620 nm and emission at 670 nm.

RESULTS

Peptide Insertion into the Micelle. The samples were prepared at high DPC (100 mM) and low gH625−644 (1 mM) concentrations to avoid peptide aggregation problems (molar ratio:peptide/DPC = 1/100). To characterize the formation of the DPC aggregates and the insertion of the ^{15}N-Ala-gH625−644 peptide into the micelles, diffusion NMR experiments were recorded. The translational diffusion coefficient, D_{trans}, measured on the peptide in the DPC solution yielded a value of $(0.87 \pm 0.01) \times 10^{-10}$ m^2/s, with a hydrodynamic Stokes radius of 29.7 ± 0.5 Å, which correspond to an aggregate with an average molecular size of 23 300 Da comprising of 55−65 detergent molecules.[33] The obtained value, which is the result of the weighted average of the diffusion coefficient of the free species and the bound species, is in good agreement with the values reported in the literature for peptides almost completely inserted into micellar aggregates,[34,35] and it is a strong indication of the interaction of the gH625−644 fusion peptide with the DPC micelle.

Assignment, Structure Calculation, and Dynamics. The NMR spectra of selectively labeled samples are very efficient in providing desired information for peptides in biomembrane mimetic solvents like micellar environments. Labeled amino acids can be easily assigned and used to obtain structural and dynamic data. In gH625−644 (NH_2−HGLASTLTRWAHYNALIRAF-COOH), alanine is the most represented amino acid; in fact, four alanine residues, Ala^{628}, Ala^{635}, Ala^{639}, and Ala^{643} are present and distributed along the sequence. This alanine distribution resulted in a favorable condition for a selective ^{15}N labeling aimed at monitoring gH625−644 behavior in a micellar environment.

^{1}H−^{15}N HSQC, homonuclear, and ^{15}N-filtered TOCSY and NOESY experiments were used to assign the ^{1}H resonances of gH625−644 and the ^{15}N chemical shifts of the four alanines.

A total of 129 NOEs were obtained from the NOESY 150 ms spectrum; these NOEs resulted in 90 meaningful distance constraints (62 interresidues, 28 intraresidues) and 85 angle

dx.doi.org/10.1021/bi201589m | *Biochemistry* 2012, 51, 3121−3128

constraints, which were used for the structure calculations. All the constraints were used to generate a total of 100 structures, among which the 20 with the lowest target function were selected and energy minimized. The obtained structures satisfied the NMR spectroscopic constraints, with no NOE violations greater than 0.2 Å. In Figure 1A, the superimposition of the 20 minimized structures is reported, whereas in Figure 1B a representative conformer is shown. gH625−644 structure is well-defined as the rmsd for residues 627−640 is 0.273 Å.

The peptide gH625−644 assumes in DPC mostly a α-helical conformation. In particular, a first helical segment encompasses residues 627−635 and is followed by a kink including residues 636−637 and a second helical region from residue 638 to 641. The angle between the two helix axes is about 100°. Interestingly, ^{15}N-Ala^{643} is not included in the structured region, but it is located in the disordered C-terminal tail.

The superposition of the crystal structure of the conserved herpes virus fusion regulator complex gH-gL from HSV type 2 (light/dark blue; PDB code 3M1C)[11] and a representative gH625−644 conformer in DPC (green) is reported (Figure 2).

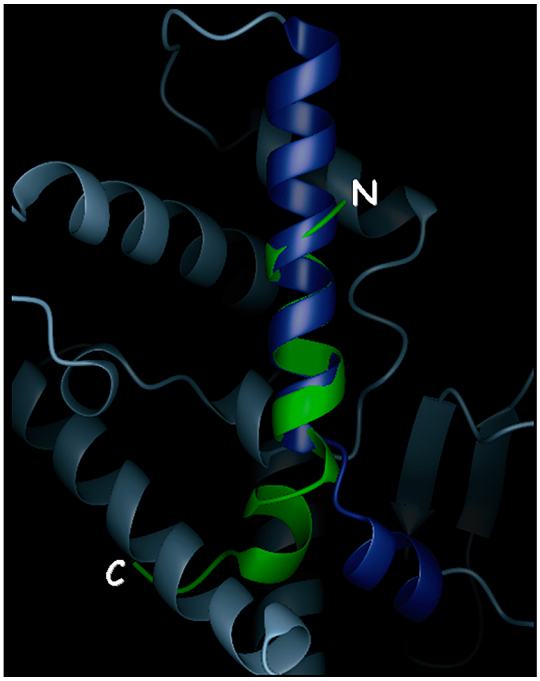

Figure 2. Superposition of the crystal structure of the conserved herpes virus fusion regulator complex gH-gL from HSV type 2 (light/dark blue; PDB code 3M1C) and a representative gH625−644 conformer in DPC (green) is reported.

Inspection of the whole protein structure reveals a α-helix for amino acids 616−635 and amino acids 638−645 (dark blue in the figure) disrupted by a two-residue kink. With the exception of three residues at the N-terminus (H625R, L627V, T630V) the HSV1 and HSV2 sequences are identical in this region. The superposition analysis demonstrates that gH625−644 is constituted by two helices separated by a kink, as observed in the whole protein. Sequences 627−635 and 638−641 maintain their helical nature even if the fragment is excised from the whole protein. A clear structural difference is observed in the angle between the helix axes that can be easily explained by considering that gH625−644 in the protein is also subject to long-range interactions determined by its tertiary structure.

Direct information on the conformational dynamics of gH625−644 have been achieved using ^{15}N{^{1}H} steady-state heteronuclear NOEs (Figure 3). Examination of the data

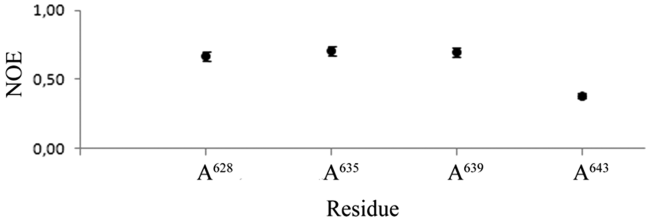

Figure 3. ^{15}N−{^{1}H} steady-state NOE for the ^{15}N-Ala-labeled gH625−644 in DPC micelles at magnetic field strength corresponding to a ^{1}H Larmor frequency of 500 MHz at 300 K.

immediately reveals a faster internal motion for the fourth alanine evidencing a different flexibility of the regions of the molecule containing the four labeled amino acids. The differences in term of internal motion clearly support the hypothesis of a different positioning of this amino acid with respect to the micelle: considering the length of the peptide and the fact that the residue is located in the disordered C-terminal tail, Ala^{643} could be partly solvent exposed.

Paramagnetic Mapping. To determine the residues of gH625−644 that are inserted into the micelle, an internal and external paramagnetic mapping was carried out on the peptide−DPC solution. $MnCl_2$ and the 16-doxyl-labeled phospholipid were used as external and internal probes, respectively. The Mn^{2+} paramagnetic probe was added to the peptide solution in different aliquots to obtain Mn^{2+}/peptide molar ratio ranging from 0.6/1 to 3/1. The Mn^{2+} addition effect was clearly visible in the HSQC spectrum (Figure 4). In particular, it affected the ^{1}H−^{15}N signal of Ala^{643}, which was subject to a large broadening; high $MnCl_2$ concentration (molar ratio $MnCl_2$/peptide 3/1) removed the Ala^{643} resonance from the spectrum. The effect of the paramagnetic probe on ^{15}N-labeled-Ala signal intensities is also reported in Figure 4 (panel D) where the intensity reduction for the four alanines at different probe concentrations is reported. As it can be seen, the paramagnetic ion induces a small effect on the first three alanines, while largely affects the resonance amplitude of Ala^{643}, supporting the above-reported hypothesis that only Ala^{643} is located outside the micelle. This finding is further supported by the disappearance in the spectrum, already at molar ratio $MnCl_2$/peptide 1/1, of the protonic resonances assigned to the backbone of amino acids Ile^{641}, Arg^{642}, Ala^{643}, and Phe^{644} located in the C-terminal tail of gH625−644. The paramagnetic relaxation enhancement also selectively affects the side chain protons of the C- terminal residues and leaves mostly unperturbed the remaining resonances.

To confirm the obtained results, residues located in the DPC micelle interior were mapped using the 16-DSA as internal paramagnetic probe. The ^{1}H resonances experienced a general line-broadening effect, with the Ile^{641}, Arg^{642}, Ala^{643}, and Phe^{644} amino acids resonances preserved from the paramagnetic effect. The ^{15}N-labeled residues behavior still differentiates Ala^{643} from the others since no visible effect was seen on its ^{1}H−^{15}N resonance. Ala^{628}, Ala^{635}, and Ala^{639} resonances resulted affected by the internal paramagnetic probe and the amplitude of their resonances decreased in a slightly different manner (Figure S2).

Quenching of Tryptophan by BrPC. The fluorescence emission of the tryptophan in presence of BrPC helped in the

dx.doi.org/10.1021/bi201589m | *Biochemistry* 2012, 51, 3121−3128

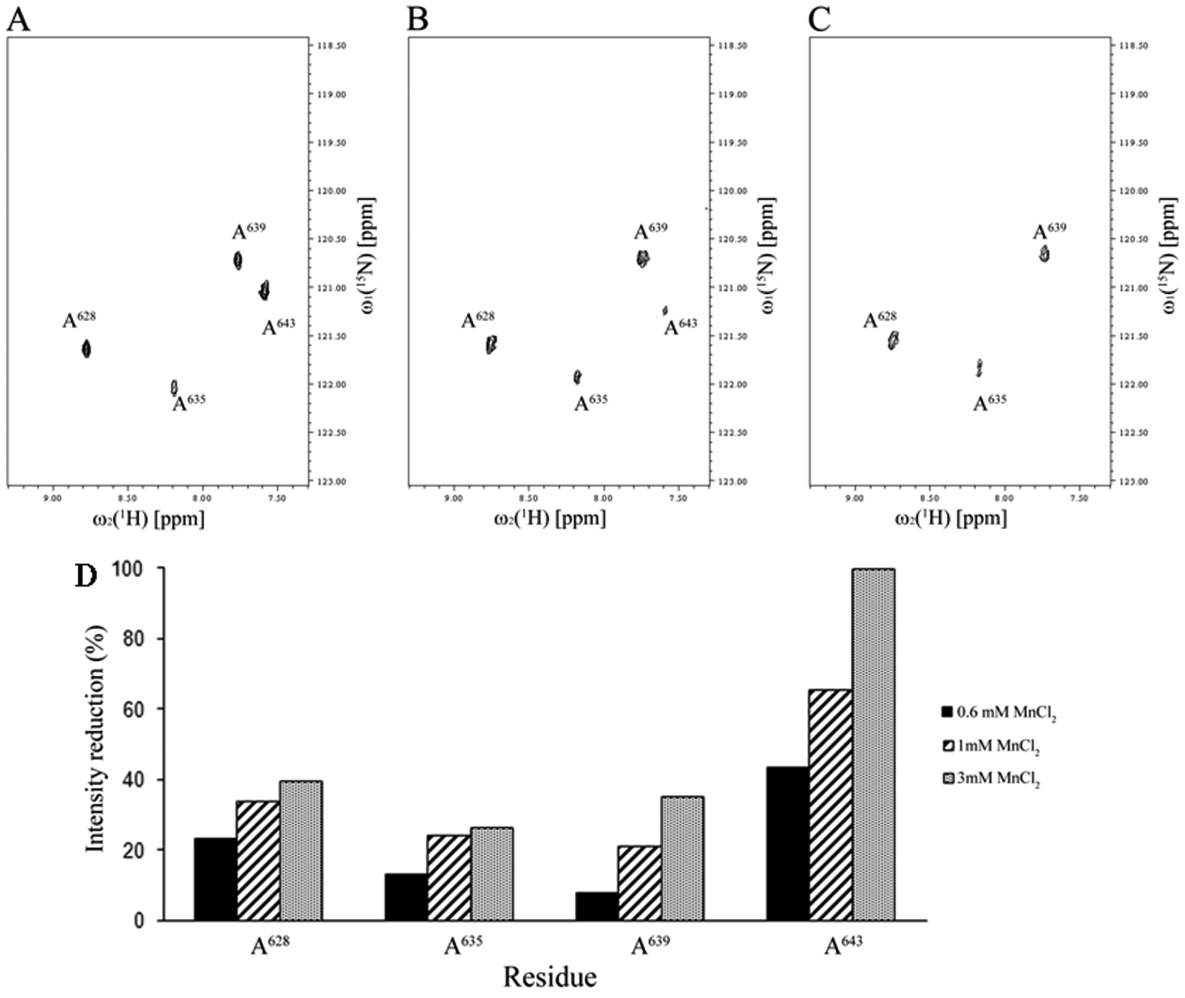

Figure 4. $^{1}H-^{15}N$ HSQC spectrum of ^{15}N-Ala-labeled gH625−644 in DPC micelles. Spectra obtained in the absence (panel A) and in the presence of 1 mM $MnCl_2$ (Mn^{2+}/peptide, 1/1) and 3 mM $MnCl_2$ (Mn^{2+}/ peptide, 3/1) (panels B and C, respectively). In panel D, the intensity reduction of $^{N}H-^{H}N$ cross-peaks in the $^{1}H-^{15}N$ HSQC spectra for the gH625−644 ^{15}N-labeled alanines at different $MnCl_2$ concentration is shown.

determination of the helix orientation. A tryptophan residue naturally present in the sequence of a protein or a peptide can serve as an intrinsic probe for the localization of the peptide within a membrane. The fluorescence emission of a tryptophan residue increases when the amino acid enters a more hydrophobic environment. This, together with an increase in quantum yield, is expected to shift the maximal spectral position toward shorter wavelengths (blue shift). Figure 5 shows the fluorescence emission spectra of the peptide gH625−644 upon interaction with PC/Chol vesicles. Changes in the spectral properties of the peptide were observed, suggesting that the tryptophan residue is located in a less polar environment upon interaction with lipids.

Furthermore, the position and the depth of the peptides inside the bilayer can be investigated by measuring the relative quenching of the fluorescence of the Trp residue by the probes 11,12-Br-PC, 9,10-Br-PC, and 6,7-Br-PC, which differ in the position of the quencher moiety along the hydrocarbon chain. 6,7-Br-PC is a better quencher for molecules near or at the interface, while the other two are better probes for molecules buried deeply in the membrane. The largest quenching of tryptophan fluorescence was observed with 11,12- Br-PC vesicles and 9,10-Br-PC (Figure 5), while slightly less quenching was observed with 6,7-Br-PC. These results clearly indicate that, upon binding to vesicles, the peptide was inserted into the membrane bilayer with the tryptophan side chain pointing toward the micelle interior.

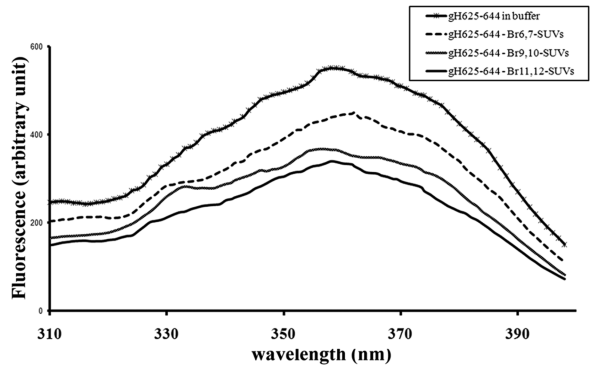

Figure 5. Tryptophan fluorescence spectra for gH625−644 in buffer and in the presence of the probes 11,12-Br-PC, 9,10-Br-PC, and 6,7-Br-PC.

Fluorometric Detection of Membrane Pores. Increasing concentrations of the peptide gH625−644 were mixed with the same amount of PC/Chol SUVs pretreated with the fluorescence dye and valinomycin. We did not evidence any enhanced recovery of fluorescence (quenched by the addition of valinomycin) after the addition of increasing amounts of

dx.doi.org/10.1021/bi201589m | *Biochemistry* 2012, 51, 3121−3128

peptide. Our results clearly indicate that there is no electroporation effect due to the peptide interactions with the SUVs.

DISCUSSION

The conformation of peptides in lipid bilayers, their orientation, and depth of insertion provide important insights into the function of membranotropic molecules; this information is particularly useful for peptides that spontaneously insert into membranes to determine the mechanism of membrane disruption and of translocation. The use of detergent micelles in such cases offers a biologically relevant environment. Moreover, numerous NMR studies on small helical peptides in micellar environment showed that peptides retain their mode of binding upon the transition from bilayers to micelles.[36,37]

The glycoprotein H (gH) is part of a multiprotein complex that enables fusion of the HSV-1 viral envelope with the host cell. In particular, the ectodomain of gH contains several regions that are required for fusion and the segment between amino acids 625−644 represents the most fusogenic region identified.[10] Here, we report the NMR solution structural characterization in a membrane-mimicking DPC micellar environment of a peptide containing residues 625−644 of gH (gH625−644) to gain insight into how gH fuses with the host cell.

Several mechanisms are currently being considered for how cell-penetrating peptides cross membrane bilayers; mainly they can proceed via either one of the two possibilities: transmembrane pore formation or membrane destabilization. This last mechanism can in turn proceed via several mechanisms such as the induction of inverse micelles, the use of an endocytic pathway or an electroporation like mechanism, or others. So far, all the data available on gH625−644 seem to indicate that this peptide is unable to form stable transmembrane pores[14] and suggest a destabilization mechanism for its penetration into the membrane bilayers.

The interactions of a peptide containing residues 626−644 of gH with the lipid bilayer have been previously studied[9,10] and indicate that the peptide penetrates deeply into the bilayer. On one hand, this argues against the models based on endocytic pathways and on the formation of inverse micelles where the peptides are associated with the bilayer surface. On the other hand, on the basis of our results, we can also exclude an electroporation-like mechanism for gH625−644 membrane penetration. So the traslocation mechanism is related to the local membrane destabilization and has to be further characterized.

gH625−644 structure in DPC shows that the peptide assumes a helical conformation beginning with residues Leu^{627} and ending at Ala^{635} followed by a kink including residues 636−637 and a final helical region from residue Asn^{638} to Ile^{641}; the polar residues concentrate on one face of the N-terminal helix, giving to it an amphiphilic character (Figures 1C,D) common to membranotropic peptides of most fusion glycoproteins of enveloped viruses. Interestingly, an amphiphilic distribution of the side chains is also observed on the C-terminal helix, but in this case the charged face is oppositely positioned with respect to the first helix, causing a clear asymmetric distribution of the peptide charges. Accordingly, the three alanines reside on the same side of the structure, but on the opposite interface of it as the Trp^{634}. The dimensions of peptide−micelle assemblies, as determined by diffusion experiments, do not indicate dimerization or formation of larger aggregates. In addition, we did not find any NOEs that do not fit a monomeric structure. Therefore, we have no indication for peptide−peptide interactions in the micelles. A paramagnetic mapping carried out on the peptide−DPC solution using $MnCl_2$ and the 16-DSA as external and internal probes respectively has allowed us to determine the residues of gH625−644 that are inserted into the micelle. The paramagnetic metal ion induces a small effect on the first three alanines, while largely affects the resonance amplitude of Ala^{643}, demonstrating that this residue is located just outside the DPC micelle. The micelle internal mapping using the 16-DSA has demonstrated how the ^{1}H resonances experimented a general line-broadening effect, with the Ile^{641}, Arg^{642}, Ala^{643}, and Phe^{644} amino acid resonances preserved from the paramagnetic effect. The ^{15}N-labeled residues behavior still differentiate Ala^{643} from the others since no visible effect was seen on its $^{1}H-^{15}N$ resonance. In contrast, Ala^{628}, Ala^{635}, and Ala^{639} resonances resulted equally affected by the internal paramagnetic probe. In addition, these last three alanines also show similar dynamic properties that again differentiate them from Ala^{643}. These data clearly demonstrate that the N-terminal part of gH625−644 is completely embedded into the DPC micelle and its C-terminal portion is outside the micelle, supporting the idea of a penetration of the micelle from the N-terminus. In fact, the asymmetrical nature of gH625−644 structure also suggests a higher ability of the N-terminus to penetrate the hydrocarbon region of the bilayer compared to the C-terminus. This result confirms the previous data indicating the penetration of this peptide from the N-terminus,[10] and it is further supported by literature data reporting that insertion of peptides from the C-terminus requires a more extensive, energetically unfavorable dehydration of the polar groups than insertion from the N-terminus.[38,39]

A defined model simulating the insertion mode of gH625−644 into the micelle based on calculated paramagnetic distances from the 16-DSA is not attainable since it would be feasible only assuming that the end of the 16-DSA is located at the center of the micelle. In the present case, 16-DSA is somehow embedded in the DPC micelle, a very dynamic environment. Given that peptide and 16-DSA were neither covalently linked, nor forming a tight 1:1 complex, statistically there will be some micelles that have two DSA molecules and some with no DSA. Since paramagnetic distances are dominated by the closest-contact distances, a quantitative distance determination cannot be derived in such a dynamic situation.

Nevertheless, considering the structure of 16-DSA, the fact that the alanines are almost equally affected by the paramagnetic probe and that our quenching experiments indicate the tryptophan side chain pointing toward the micelle interior, a reliable cartoon of the peptide orientation can be drawn: the N-terminal part of gH625−644 is completely embedded into the DPC micelle and lies approximately parallel to the micelle surface (Figure 6) while the C-terminal portion resides outside the micelle.

In conclusion, we have found that gH625−644 binds as a monomer to zwitterionic membrane mimetics. The three-dimensional structure has evidenced an amphiphilic character of this peptide and, more importantly, a strong asymmetric distribution of the peptide positive charges. The sequence requirements for the gH625−644 peptide to penetrate membranes have been previously investigated using a wide range of designed sequence variants and have generally established that a net positive charge at the C-terminus is

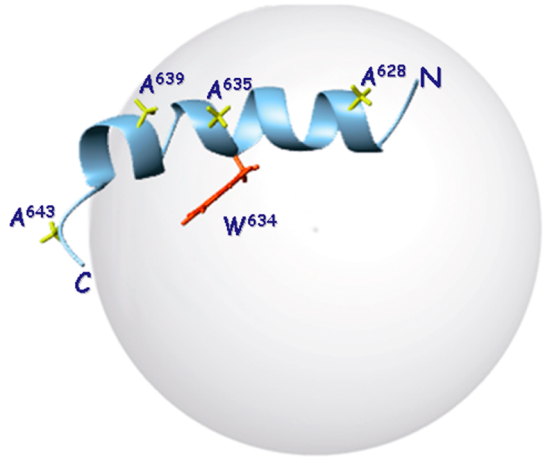

Figure 6. Cartoon representing the possible insertion mode of gH625−644 in DPC micelles. The alanine side chains are shown in yellow while the tryptophan side chain is colored pink.

needed for membrane binding. Moreover, it has been shown that the tryptophan is required for membrane penetration and that an histidine and a glycine at the N-terminus are fundamental for fusion activity.[10] The data here reported further support the hypothesis that binding of gH625−644 to the hydrophilic region of lipid headgroups is mediated by both the basic and aromatic amino acids; deep penetration of the peptide is thus correlated with the hydrophobicity of the sequence and its amphiphilicity. The function of the aromatic residues is to cause the peptide insertion into the membrane interface while the basic residues stabilize this interaction by linking the negatively charged headgroups as shown in other systems using both NMR[40,41] and EPR.[42] Therefore, our model emphasizes that both electrostatic and hydrophobic interactions work in concert to mediate membrane penetration.

■ ASSOCIATED CONTENT

Ⓢ Supporting Information

Two figures reporting the "summary of short and medium range NOEs for gH625−644" and "signal reduction of the alanine amide protons induced by the external paramagnetic probe". This material is available free of charge via the Internet at http://pubs.acs.org.

■ AUTHOR INFORMATION

Corresponding Author

*Tel: +39 0823 274636; Fax: +39 0823 274605; e-mail: carla.isernia@unina2.it.

Author Contributions

#Stefania Galdiero and Luigi Russo contributed equally to the work.

Funding

This work was partially funded by M.I.U.R. Grants PRIN 2007 (to C.I.) and PRIN 2008 (to R.F.).

Notes

The authors declare no competing financial interest.

■ ACKNOWLEDGMENTS

We thank Dr. Luca Raiola for useful discussions as well as Mr. Maurizio Muselli and Mr. Leopoldo Zona for excellent technical assistance.

■ REFERENCES

(1) Harrison, S. C. (2008) Viral membrane fusion. *Nat. Struct. Mol. Biol. 15*, 690−698.
(2) Campadelli-Fiume, G., Amasio, M., Avitabile, E., Cerretani, A., Forghieri, C., Gianni, T., and Menotti, L. (2007) The multipartite system that mediates entry of herpes simplex virus into the cell. *Rev. Med. Virol. 17*, 313−326.
(3) Spear, P. G., and Longnecker, R. (2003) Herpesvirus entry: an update. *J. Virol. 77*, 10179−10185.
(4) Turner, A., Bruun, B., Minson, T., and Browne, H. (1998) Glycoproteins gB, gD, and gHgL of herpes simplex virus type 1 are necessary and sufficient to mediate membrane fusion in a Cos cell transfection system. *J. Virol. 72*, 873−875.
(5) Shukla, D., and Spear, P. G. (2001) Herpesviruses and heparan sulfate: an intimate relationship in aid of viral entry. *J. Clin. Invest. 108*, 503−510.
(6) Jackson, J. O., and Longnecker, R. (2010) Reevaluating herpes simplex virus hemifusion. *J. Virol. 84*, 11814−11821.
(7) Heldwein, E. E., Lou, H., Bender, F. C., Cohen, G. H., Eisenberg, R. J., and Harrison, S. C. (2006) Crystal structure of glycoprotein B from herpes simplex virus 1. *Science 313*, 217−220.
(8) Galdiero, M., Whiteley, A., Bruun, B., Bell, S., Minson, T., and Browne, H. (1997) Site-directed and linker insertion mutagenesis of herpes simplex virus type 1 glycoprotein H. *J. Virol. 71*, 2163−2170.
(9) Galdiero, S., Falanga, A., Vitiello, M., Raiola, L., Fattorusso, R., Browne, H., Pedone, C., Isernia, C., and Galdiero, M. (2008) Analysis of a membrane interacting region of herpes simplex virus type 1 glycoprotein H. *J. Biol. Chem. 283*, 29993−30009.
(10) Galdiero, S., Falanga, A., Vitiello, M., Raiola, L., Russo, L., Pedone, C., Isernia, C., and Galdiero, M. (2010) The presence of a single N-terminal histidine residue enhances the fusogenic properties of a Membranotropic peptide derived from herpes simplex virus type 1 glycoprotein H. *J. Biol. Chem. 285*, 17123−17136.
(11) Chowdary, T. K., Cairns, T. M., Atanasiu, D., Cohen, G. H., Eisenberg, R. J., and Heldwein, E. E. (2010) Crystal structure of the conserved herpesvirus fusion regulator complex gH-GL. *Nat. Struct. Mol. Biol. 17*, 882−888.
(12) Atanasiu, D., Whitbeck, J. C., de Leon, M. P., Lou, H., Hannah, B. P., Cohen, G. H., and Eisenberg, R. J. (2010) Bimolecular complementation defines functional regions of Herpes simplex virus gB that are involved with gH/gL as a necessary step leading to cell fusion. *J. Virol. 84*, 3825−3834.
(13) Galdiero, S., Falanga, A., Vitiello, M., Browne, H., Pedone, C., and Galdiero, M. (2005) Fusogenic domains in herpes simplex virus type 1 glycoprotein H. *J. Biol. Chem. 280*, 28632−28643.
(14) Falanga, A., Vitiello, M., Cantisani, M., Tarallo, R., Guarnieri, D., Mignogna, E., Netti, P., Pedone, C., Galdiero, M., and Galdiero, S. (2011) A peptide derived from herpes simplex virus type 1 glycoprotein H: membrane translocation and applications to the delivery of quantum dots. *Nanomedicine 7*, 925−934.
(15) Tarallo, R., Accardo, A., Falanga, A., Guarnieri, D., Vitiello, G., Netti, P., D'Errico, G., Morelli, G., and Galdiero, S. (2011) Clickable Functionalization of Liposomes with the gH625 Peptide from Herpes simplex Virus Type I for Intracellular Drug Delivery. *Chem.—Eur. J. 17*, 12659−12668.
(16) le Maire, M., Champeil, P., and Møller, J. V. (2000) Interaction of membrane proteins and lipids with solubilizing detergents. *Biochim. Biophys. Acta 1508*, 86−111.
(17) Griesinger, C., Otting, G., Wüthrich, K., and Ernst, R. R. (1988) Clean TOCSY for 1H spin system identification in macromolecules. *J. Am. Chem. Soc. 110*, 7870−7872.
(18) Kumar, A., Ernst, R. R., and Wüthrich, K. (1980) A two-dimensional nuclear Overhauser enhancement (2D NOE) experiment for the elucidation of complete proton-proton cross-relaxation networks in biological macromolecules. *Biochem. Biophys. Res. Commun. 95*, 1−6.
(19) Hwang, T. L., and Shaka, J. (1995) Water Suppression That Works. Excitation Sculpting Using Arbitrary Wave-Forms and Pulsed-Field Gradients. *J. Magn. Reson., Ser. A 112*, 275−279.

(20) Keller, R. (2004) *The Computer Aided Resonance Assignment Tutorial*, CANTINA Verlag Goldau.
(21) Güntert, P. (2004) Automated NMR structure calculation with CYANA. *Methods Mol. Biol. 278*, 353−378.
(22) Herrmann, T., Güntert, P., and Wüthrich, K. (2002) Protein NMR structure determination with automated NOE assignment using the new software CANDID and the torsion angle dynamics algorithm DYANA. *J. Mol. Biol. 319*, 209−227.
(23) Guex, N., and Peitsch, M. C. (1997) SWISS-MODEL and the Swiss-PdbViewer: an environment for comparative protein modeling. *Electrophoresis 18*, 2714−2723.
(24) Koradi, R., Billeter, M., and Wüthrich, K. (1996) MOLMOL: a program for display and analysis of macromolecular structures. *J. Mol. Graphics 14*, 29−32.
(25) Laskowski, R. A., Rullmann, J. A., MacArthur, M. W., Kaptein, R., and Thornton, J. M. (1996) AQUA and PROCHECK-NMR: programs for checking the quality of protein structures solved by NMR. *J. Biomol. NMR 8*, 477−486.
(26) Gibbs, S. J., and Johnson, C. S. Jr. (1991) A PFG NMR experiment for accurate diffusion and flow studies in the presence of eddy currents. *J. Magn. Reson. 93*, 395−402.
(27) Wilkins, D. K., Grimshaw, S. B., Receveur, V., Dobson, C. M., Jones, J. A., and Smith, L. J. (1999) Hydrodynamic radii of native and denatured proteins measured by pulse field gradient NMR techniques. *Biochemistry 38*, 16424−16431.
(28) de la Torre, J. G., Huertas, M. L., and Carrasco, B. (2000) Calculation of Hydrodynamic Properties of Globular Proteins from Their Atomic-Level Structure. *Biophys. J. 78*, 719−730.
(29) Bolen, E. J., and Holloway, P. W. (1990) Quenching of tryptophan fluorescence by brominated phospholipid. *Biochemistry 29*, 9638−9643.
(30) De Kroon, A. I., Soekarjo, M. W., De Gier, J., and De Kruijff, B. (1990) The role of charge and hydrophobicity in peptide-lipid interaction: a comparative study based on tryptophan fluorescence measurements combined with the use of aqueous and hydrophobic quenchers. *Biochemistry 29*, 8229−8240.
(31) Sims, P. J., Waggoner, A. S., Wang, C. H., and Hoffman, J. R. (1974) Studies on the mechanism by which cyanine dyes measure membrane potential in red blood cells and phosphatidylcholine vesicles. *Biochemistry 13*, 3315−3330.
(32) Shai, Y., Bach, D., and Yanovsky, A. (1990) Channel formation properties of synthetic pardaxin and analogues. *J. Biol. Chem. 265*, 20202−20209.
(33) Groves, P., Rasmussen, M. O., Molero, M. D., Samain, E., Cañada, F. J., Driguez, H., and Jimenez-Barbero, J. (2004) Diffusion ordered spectroscopy as a complement to size exclusion chromatography in oligosaccharide analysis. *Glycobiology 14*, 451−456.
(34) Shenkarev, Z. O., Balashova, T. A., Efremov, R. G., Yakimenko, Z. A., Ovchinnikova, T. V., and Raap, J. (2002) Spatial structure of Zervamicin IIB bound to DPC micelles: Implications for voltage-gating. *Biophys. J. 82*, 762−771.
(35) Gao, X., and Wong, T. C. (1998) Studies of the binding and structure of adrenocorticotropin peptides in membrane mimics by NMR spectroscopy and pulsed-field gradient diffusion. *Biophys. J. 74*, 1871−1888.
(36) Opella, S. J., Kim, Y., and McDonnell, P. (1994) Experimental nuclear magnetic resonance studies of membrane proteins. *Methods Enzymol. 239*, 536−560.
(37) Pervushin, K. V., and Arseniev, A. S. (1995) NMR spectroscopy in the study of the spatial structure of membrane peptides and proteins. *Bioorg. Khim. 21*, 83−111.
(38) Ben-Tal, N., Ben-Shaul, A., Nicholls, A., and Honig, B. (1996) Free-energy determinants of alpha-helix insertion into lipid bilayers. *Biophys. J. 70*, 1803−1812.
(39) Chipot, C., and Pohorille, A. (1998) Folding and translocation of the undecamer of poly-L-leucine across the water-hexane interface. A molecular dynamics study. *J. Am. Chem. Soc. 120*, 11912−11924.
(40) Zhang, W., Crocker, E., McLaughlin, S., and Smith, S. O. (2003) Binding of peptides with basic and aromatic residues to bilayer membranes: phenylalanine in the myristoylated alanine-rich C kinase substrate effector domain penetrates into the hydrophobic core of the bilayer. *J. Biol. Chem. 278*, 21459−21466.
(41) Jing, W., Hunter, H. N., Hagel, J., and Vogel, H. J. (2003) The structure of the antimicrobial peptide Ac-RRWWRF-NH2 bound to micelles and its interactions with phospholipid bilayers. *J. Pept. Res. 61*, 219−229.
(42) Rauch, M. E., Ferguson, C. G., Prestwich, G. D., and Cafiso, D. S. (2002) Myristoylated alanine-rich C kinase substrate (MARCKS) sequesters spin-labeled phosphatidylinositol 4,5-bisphosphate in lipid bilayers. *J. Biol. Chem. 277*, 14068−14076.